Energy Transfer

DOI: 10.1002/ange.201208514

A Photoconductive Thienothiophene-Based Covalent Organic Framework Showing Charge Transfer Towards Included Fullerene**

Mirjam Dogru, Matthias Handloser, Florian Auras, Thomas Kunz, Dana Medina, Achim Hartschuh, Paul Knochel, and Thomas Bein**

Organic bulk heterojunctions combining electron donor and acceptor phases are of great interest for designing organic photovoltaic devices.[1] While impressive advances have been achieved with these systems, so far a deterministic control of their nanoscale morphology has been elusive. It would be a major breakthrough to be able to create model systems with periodic, interpenetrating networks of electron donor and acceptor phases providing maximum control over all structural and electronic features.

Herein we report a significant step towards this goal on the basis of the recently discovered class of crystalline covalent organic frameworks (COFs) which are created by condensation of molecular building blocks.[2–5] Specifically, the stacked layers of two-dimensional COFs permit charge migration through the framework,[6] and several semiconducting structures[7] with high carrier mobilities[8–10] have been described. We have created a COF containing stacked thieno[2,3-b]thiophene-based building blocks serving as electron donors (TT-COF), with high surface area and a 3 nm open pore system. This open framework takes up the well-known fullerene electron acceptor [6,6]-phenyl-C_{61}-butyric acid methyl ester (PCBM), thus forming a novel structurally ordered donor–acceptor network. Spectroscopic results demonstrate light-induced charge transfer from the photoconductive TT-COF donor network to the encapsulated PCBM phase in the pore system. Moreover, we have created the first working COF-based photovoltaic device with the above components. The organization of the molecular building blocks into a crystalline framework with defined conduction paths provides a promising model system for ordered and interpenetrated networks of donors and acceptors at the nanoscale.

The most prominent hole-conducting material used in organic solar cells is poly(3-hexylthiophene) (P3HT), a thiophene-containing polymer with high charge-carrier mobilities. The soluble fullerene derivative PCBM is often used as an electron acceptor in organic photovoltaics.[11] Because of the lack of structural order in the respective bulk heterojunctions it is very difficult to assess the impact of molecular building blocks, bonding motifs, and energy levels on the microscopic processes involving light-induced exciton formation, charge separation, and transport in such systems. Hence ordered charge-transporting networks with a periodicity of several nanometers are of great interest to understand the mechanistic details of the light-induced processes and ultimately to obtain design rules for the creation of efficient and stable organic photovoltaic devices.[12,13]

The new TT-COF was synthesized under solvothermal conditions by co-condensation of thieno[3,2-b]thiophene-2,5-diyldiboronic acid (TTBA) and the polyol 2,3,6,7,10,11-hexahydroxytriphenylene (HHTP; Figure 1a). Reaction parameters are described in the Supporting Information.

As described in the following, the thienothiophene-based COF forms stacks in an AA arrangement, as confirmed by N_2 sorption and powder X-ray diffraction.

Powder X-ray diffraction (PXRD) confirms the formation of a highly crystalline COF. Identification of the new structure was conducted by comparison of structures modeled with MS Studio (see Figures S1–S5 in the Supporting Information).[14] Corresponding powder patterns were simulated and compared to the experimentally obtained data. For previous COF structures different stacking types of the hexagonal planar sheets were reported.[1] Hence calculations were carried out simulating an eclipsed AA arrangement and a staggered AB arrangement. The experimental PXRD pattern for TT-COF agrees very well with the simulated pattern for an eclipsed AA arrangement (Figure 1b) with a hexagonal *P6m* symmetry. Moreover, unit-cell parameters determined from the experimental X-ray patterns match very well with those obtained from the structure simulations (peak broadening included). FT-IR spectroscopy can confirm the presence of the newly formed boronate ester functionality. As previously reported, the attenuation of the OH stretching band resulting from the ester formation is apparent, and furthermore the most characteristic modes of the C-B and C-O functionalities can be assigned to the bands at 1395 cm^{-1} and 1353 cm^{-1} (see Figure S8 in the Supporting Information).[15]

The ^{11}B MAS NMR spectrum (see Figure S9 in the Supporting Information) shows a trigonal-planar boron atom with a chemical shift of $\delta = 21$ ppm, which can be distinguished from the starting material (TTBA: $\delta = 15$ ppm). Transmission electron microscopy (TEM) images show the nanoscale morphology of the crystals. A slightly tilted side view shows the long ordered channels with distinct pore sizes (see Figure S12 in the Supporting Information). A top view

[*] Dr. M. Dogru, M. Handloser, F. Auras, Dr. T. Kunz, Dr. D. Medina, Prof. Dr. A. Hartschuh, Prof. Dr. P. Knochel, Prof. Dr. T. Bein
Department of Chemistry and Center for NanoScience (CeNS), Ludwig-Maximilians-Universität Munich (LMU)
Butenandtstraße 5–13 (E), 81377 Munich (Germany)
E-mail: knoch@cup.uni-muenchen.de
bein@lmu.de
Homepage: http://www.bein.cup.uni-muenchen.de

[**] The authors gratefully acknowledge funding from the NIM excellence cluster (DFG). We thank Bastian Rühle for 3D graphics and Markus Döblinger for transmission electron microscopy.

Supporting information for this article is available on the WWW under http://dx.doi.org/10.1002/anie.201208514.

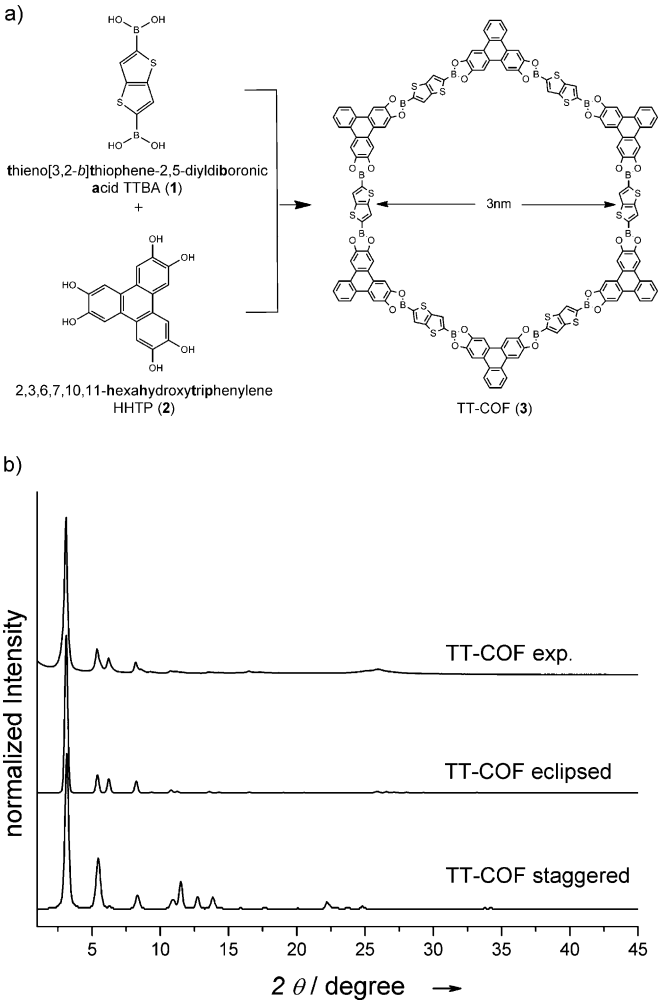

Figure 1. a) Reaction scheme for the co-condensation of TT-COF. b) Comparison of the experimentally observed PXRD pattern (top) with the simulated patterns using the module Reflex of MS Studio in an AA arrangement (middle) and AB arrangement (bottom).

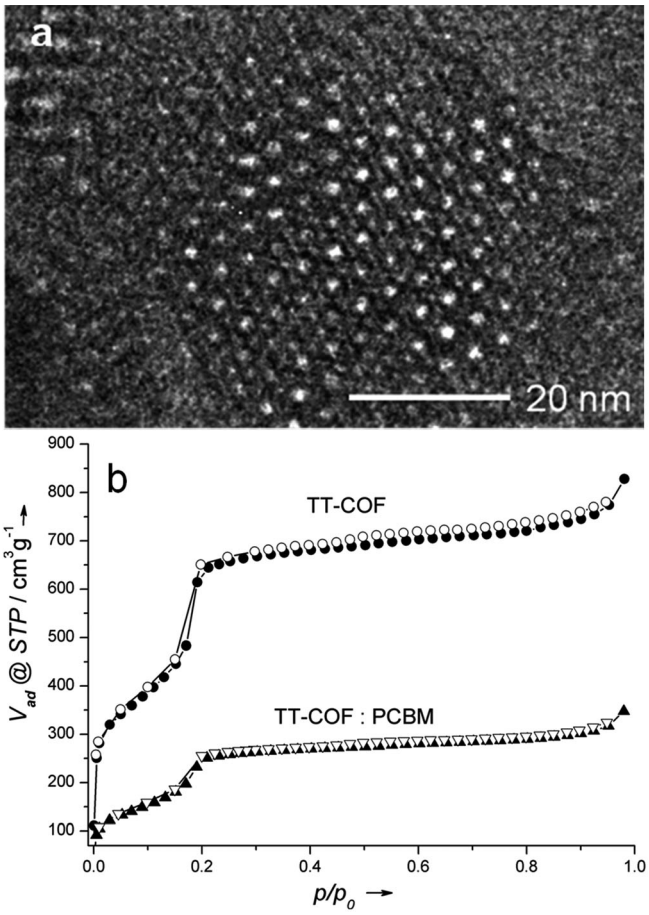

Figure 2. a) TEM micrograph (top view) along the c-axis showing the hexagonal structure of TT-COF. b) Nitrogen sorption isotherm of degassed TT-COF measured at 77 K (●: adsorption ○: desorption) and TT-COF:PCBM (▲: adsorption △ : desorption).

along the c-axis shows hexagonal structures with a pore-to-pore distance of around 3 nm (Figure 2a). The morphology identified by TEM can be ascertained by scanning electron microscopy (SEM), which shows small crystals with sizes of about 100 nm that grow into larger arrangements (see Figure S13 in the Supporting Information). Based on peak broadening of the PXRD patterns we obtain an average domain size of about 30 nm.

The porosity of TT-COF was confirmed with N_2 sorption measurements at 77 K. The obtained type IV isotherm is characteristic for mesoporous materials (Figure 2b), and shows a very well-defined jump in the uptake as a result of the highly crystalline mesoporous pore system. The very high Brunauer-Emmett-Teller (BET) surface area was calculated to be 1810 m^2g^{-1} and the pore volume is 1.19 cm^3g^{-1}. Evaluation of the isotherm using the NLDFT-based kernel gives a pore size of 3 nm (see Figure S7 in the Supporting Information). The experimentally obtained surface area and pore volumes from the sorption data were compared to theoretical values obtained with the Connolly method and they are in good agreement (Table 1). In crystalline materials these values can be predicted using geometric methods.[16,17] Based on these results we can conclude that the pores of TT-COF are not blocked by solvent molecules or by oligomeric fragments.

Table 1: Theoretical and experimental values for surface area and pore volume of TT-COF.

	Pore size [nm]	Surface area [m^2g^{-1}]	Pore volume [cm^3g^{-1}]
TT-COF	3.0	1810	1.19
Connolly	3.0	1810	1.17
TT-COF:PCBM	2.4	700	0.49

All these results demonstrate that TT-COF is a well-defined mesoporous crystalline material with highly organized sheets resulting in high surface areas. Semiconducting polymers based on the thieno[2,3-b]thiophene building block are known and these polymers exhibit high charge-carrier mobilities and are stable under ambient conditions.[18] Moreover, photoinduced charge transfer from polymerized thie-

nothiophene derivatives to fullerene-based acceptor molecules is known.[19] This prompted us to study the electronic interactions between TT-COF and PCBM. The large pores of TT-COF allow for the uptake of the fullerene molecules (because of attractive van der Waals interactions between the host and the guest molecules) and thus for the investigation of the resulting host–guest interactions (Figure 3).

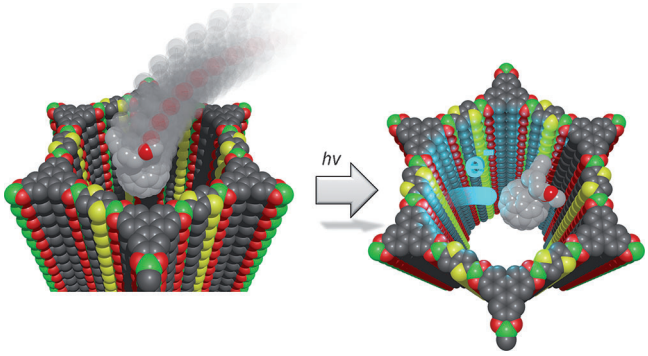

Figure 3. Schematic representation of the host–guest complex of TT-COF and a PCBM molecule to scale (C grey, O red, B green, and S yellow. For clarity only one PCBM molecule is shown, whereas in the experiments described, the COF channels are loaded with the PCBM phase.

Figure 2b shows a significant reduction of the absorbed amount of nitrogen after loading TT-COF with PCBM. The BET surface area of pure TT-COF decreases from 1800 $m^2 g^{-1}$ to 700 $m^2 g^{-1}$ for TT-COF:PCBM. Furthermore, the average pore size distribution shows a broad range of pores up to 3 nm (see Figure S7 in the Supporting Information).

The pore volume decreases significantly from 1.19 $cm^3 g^{-1}$ to 0.49 $cm^3 g^{-1}$ (see Table 1). Furthermore, we evaluated the amount of PCBM adsorbed in the TT-COF using UV/Vis spectroscopy (see Figure S17 in the Supporting Information). From a 16 mg mL^{-1} PCBM solution in chlorobenzene 1.7 mg PCBM are adsorbed into 5 mg COF. Normalizing the amount adsorbed obtained by UV/Vis measurements to 1 g of TT-COF would give an uptake of 340 mg of PCBM. Thus the pore volume of TT-COF:PCBM should be corrected by the amount of PCBM (a factor of 1.34), and this results in a pore volume of 0.66 $cm^3 g^{-1}$ of TT-COF. Therefore 0.53 cm^3 of the volume is displaced by PCBM. The calculated density for 0.53 cm^3 PCBM is 0.64 g cm^{-3}, half of the bulk crystal density (1.3 g cm^{-3}), thus indicating that PCBM is not densely packed in the 3 nm pores of TT-COF.

The absorption spectra obtained for thin films of pure TT-COF, TT-COF:PCBM, and PCBM (see Figure S18 in the Supporting Information) confirm the existence of the small thienothiophene and triphenylene units in the framework. The notable optical density over the full visible spectrum is partially caused by light scattering.[20] The fluorescence emission spectrum of TT-COF shows that the framework exhibits a blue emission upon excitation at $\lambda = 380$ nm (Figure 4a). Blue-emissive polymers based on boronate ester condensation have been described by Lavigne et al., and recently the blue-emissive TP-COF has been reported.[15] Once the electron acceptor PCBM is loaded into the TT-COF, the emission band at $\lambda = 487$ nm is completely quenched. In the literature, very efficient light-induced electron transfer on the order of femtoseconds has been reported for PCBM:P3HT blends.[19] In the PCBM:TT-COF system, the photoinduced charges can dissociate at the nanostructured interface between TT-COF and PCBM. In bulk heterojunctions, short diffusion pathways on the order of 10–20 nm are necessary to reach the electron acceptor PCBM within the lifetime of the photoinduced charges.[22,23] Given the ordered nanochannels of the donor material TT-COF, having about 3 nm channel diameter and thin molecular walls, such short diffusion pathways are clearly available in the interpenetrating system PCBM:TT-COF. Therefore the observation of PL-quenching confirms the interpenetrated structure of TT-COF and PCBM.

Time-resolved photoluminescence (PL) was studied to learn more about the light-induced interactions between the TT-COF host and PCBM. The PL transients and their respective fit-functions of PCBM and TT-COF loaded with PCBM are shown in Figure 4b. In the bulk, PCBM shows bi-exponential PL decay on the nanosecond time scale, while TT-COF decays tri-exponentially with an average lifetime of 117 ps (Table 2).

Table 2: PL-lifetimes of the decay components of PCBM, PCBM:TT-COF and TT-COF.

	Average lifetime (intensity weighted)	Lifetime exp.1	Lifetime exp.2	Lifetime exp.3	PL decay
TT-COF	117 ps	191 ps (38%)	54 ps (14%)	13 ps (48%)	Tri-exp.
PCBM	1206 ps	1406 ps (76%)	794 ps (24%)		Bi-exp.
PCBM:TT-COF		1070 ps (45%)	46 ps (12%)	18 ps (43%)	Tri-exp.

When included in the channels of TT-COF, the PCBM contribution can be modeled by a single exponential decay component of 1070 ps, which is close to the intensity weighted average lifetime of 1206 ps of the bulk material. Importantly, the decay of TT-COF with a lifetime below 50 ps (46 and 18 ps) is substantially faster than the average decay in the bulk, thus indicating an efficient additional relaxation channel in agreement with the quenching observed in the PL-spectra (see Figure 4a).[24]

To further explore the capabilities of the TT-COF:PCBM sytem, we incorporated a COF film of about $d = 200$ nm thickness into a ITO/TT-COF:PCBM/Al device structure. Spincoating a rather concentrated PCBM solution on the COF film not only leads to filling of the COF pores, but also produces an overlayer, which ensures that the aluminium top contact does not short-circuit the cell. Under simulated AM1.5G full sun illumination we measured an open-circuit voltage of 622 mV, a short-circuit current density of 0.213 mA cm^{-2}, and 40% fill factor, thus giving rise to a power conversion efficiency of 0.053% (Figure 4c). Illumi-

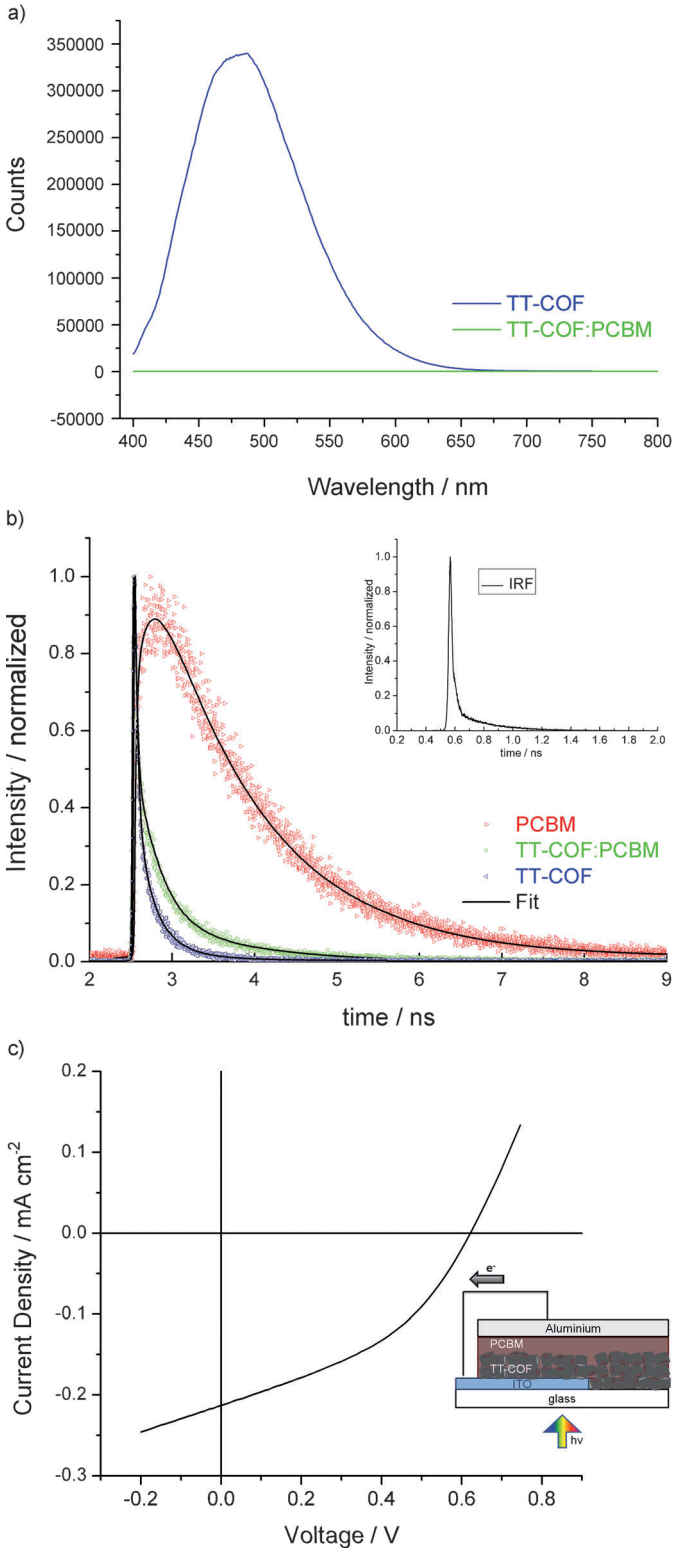

Figure 4. a) Fluorescence emission of TT-COF (blue) upon excitation at $\lambda = 380$ nm. The fluorescence of TT-COF filled with PCBM (green) is quenched. b) PL-lifetime transients of PCBM (red symbols), TT-COF (blue symbols) and PCBM:TT-COF (green symbols) thin films using a TCSPC technique under femtosecond pulsed excitation at $\lambda = 800$ nm. c) *I–V* characteristics of the TT-COF-based photovoltaic cell measured under illumination with simulated solar light.

nation density-dependent *I–V* measurements (see Figure S15 in the Supporting Information) prove that the current scales almost linearly with the light intensity. The external quantum efficiency of the device (see Figure S16 in the Supporting Information), that is, the number of extracted electrons per number of incident photons, reveals that the majority of the photocurrent is generated from wavelengths below $\lambda = 530$ nm, which is in line with the absorption spectrum of the COF film. A maximum EQE of 3.4% is observed at $\lambda = 405$ nm. The tail at longer wavelengths exhibits the characteristic feature of PCBM above $\lambda = 700$ nm, which indicates that both interpenetrating networks are photoelectrically active.

Structural disorder of the donor and the acceptor phases can limit charge-carrier mobility and the charge separation in organic bulk heterojunctions and hence can decrease the performance of organic solar cells. The creation of a crystalline semiconducting framework such as a hole transporter whose pores can be filled with the respective acceptor might ultimately overcome these limitations. The novel thienothiophene-based TT-COF described herein exhibits a significant photoresponse. Furthermore, the TT-COF structure is thermally stable and can be handled under ambient conditions. To increase the efficiency of organic solar cells it would be desirable to overcome the disadvantage of the very short exciton diffusion lengths in organic polymers like PCBM, P3HT, or MDMO-PPV. The novel interpenetrated TT-COF:PCBM structure presented herein (where the distance between the donor network and the acceptor phase is only a few nm) supports efficient charge transfer within the lifetime of the excitons. First studies of a COF-based photovoltaic device with an electron donor in the walls and the complementary electron acceptor in ordered periodic channels show that light-induced charge-separation and collection is clearly feasible with these systems. Hence we propose that interpenetrated networks of crystalline porous semiconducting COFs with electron acceptor phases such as PCBM present promising model architectures for the understanding and further development of efficient photovoltaic devices.

Received: October 22, 2012
Published online: February 4, 2013

Keywords: boron · covalent organic frameworks · energy transfer · fullerenes · photoconductivity

[1] A. P. Côté, A. I. Benin, N. W. Ockwig, M. O'Keeffe, A. J. Matzger, O. M. Yaghi, *Science* **2005**, *310*, 1166 – 1170.
[2] H. M. El-Kaderi, J. R. Hunt, J. L. Mendoza-Cortes, A. P. Côté, R. E. Taylor, M. O'Keeffe, O. M. Yaghi, *Science* **2007**, *316*, 268 – 272.
[3] A. P. Côté, H. M. El-Kaderi, H. Furukawa, J. R. Hunt, O. M. Yaghi, *J. Am. Chem. Soc.* **2007**, *129*, 12914 – 12915.
[4] E. L. Spitler, J. W. Colson, F. J. Uribe-Romo, A. R. Woll, M. R. Giovino, A. Saldivar, W. R. Dichtel, *Angew. Chem.* **2012**, *124*, 2677 – 2681; *Angew. Chem. Int. Ed.* **2012**, *51*, 2623 – 2627.

[5] X. Feng, X. Ding, D. Jiang, *Chem. Soc. Rev.* **2012**, *41*, 6010 – 6022.
[6] S. Wan, J. Guo, J. Kim, H. Ihee, D. Jiang, *Angew. Chem.* **2009**, *121*, 3253; *Angew. Chem. Int. Ed.* **2009**, *48*, 3207.
[7] S. Wan, J. Guo, J. Kim, H. Ihee, D. Jiang, *Angew. Chem.* **2009**, *121*, 5547 – 5550; *Angew. Chem. Int. Ed.* **2009**, *48*, 5439 – 5442.
[8] X. Ding, J. Guo, X. Feng, Y. Honsho, J. Guo, S. Seki, P. Maitarad, A. Saeki, S. Nagase, D. Jiang, *Angew. Chem.* **2011**, *123*, 1325 – 1329; *Angew. Chem. Int. Ed.* **2011**, *50*, 1289 – 1293.
[9] S. Wan, F. Gándara, A. Asano, H. Furukawa, A. Saeki, S. K. Dey, L. Liao, M. W. Ambrogio, Y. Y. Botros, X. Duan, S. Seki, J. F. Stoddart, O. M. Yaghi, *Chem. Mater.* **2011**, *23*, 4094 – 4097.
[10] X. Feng, L. Chen, Y. Honsho, O. Saengsawang, L. Liu, L. Wang, A. Saeki, S. Irle, S. Seki, Y. Dong, D. Jiang, *Adv. Mater.* **2012**, *24*, 3026 – 3031.
[11] G. Dennler, M. C. Scharber, C. J. Brabec, *Adv. Mater.* **2009**, *21*, 1323 – 1338.
[12] G. Yu, J. Gao, J. C. Hummelen, F. Wudl, A. J. Heeger, *Science* **1995**, *270*, 1789 – 1791.
[13] J. Peet, J. Y. Kim, N. E. Coates, W. L. Ma, D. Moses, A. J. Heeger, G. C. Bazan, *Nat. Mater.* **2007**, *6*, 497 – 500.
[14] Accelrys MS Modeling 4.4 **2008**.
[15] R. W. Tilford, W. R. Gemmill, H.-C. zur Loye, J. J. Lavigne, *Chem. Mater.* **2006**, *18*, 5296 – 5301.
[16] A. R. Leach, *Molecular Modelling: Principles and Applications*, 2nd ed., Prentice Hall, Harlow, England, **2001**.
[17] M. Connolly, *J. Appl. Crystallogr.* **1983**, *16*, 548 – 558.
[18] M. Heeney, C. Bailey, K. Genevicius, M. Shkunov, D. Sparrowe, S. Tierney, I. McCulloch, *J. Am. Chem. Soc.* **2005**, *127*, 1078 – 1079.
[19] T. J. Savenije, W. J. Grzegorczyk, M. Heeney, S. Tierney, I. McCulloch, L. D. A. Siebbeles, *J. Phys. Chem. C* **2010**, *114*, 15116 – 15120.
[20] E. L. Spitler, B. T. Koo, J. L. Novotney, J. W. Colson, F. J. Uribe-Romo, G. D. Gutierrez, P. Clancy, W. R. Dichtel, *J. Am. Chem. Soc.* **2011**, *133*, 19416 – 19421.
[21] Y. Xie, Y. Li, L. Xiao, Q. Qiao, R. Dhakal, Z. Zhang, Q. Gong, D. Galipeau, X. Yan, *J. Phys. Chem. C* **2010**, *114*, 14590 – 14600.
[22] D. Duché, E. Drouard, J. J. Simon, L. Escoubas, P. Torchio, J. Le Rouzo, S. Vedraine, *Sol. Energy Mater.* **2011**, *95*, 18 – 25.
[23] J. E. Kroeze, T. J. Savenije, M. J. W. Vermeulen, J. M. Warman, *Phys. Chem. B* **2003**, *107*, 7696 – 7705.
[24] N. S. Sariciftci, L. Smilowitz, A. J. Heeger, F. Wudl, *Science* **1992**, *258*, 1474 – 1476.

